

**A. Yu. Kaplin<sup>1</sup>, M. G. Stepanov<sup>1</sup>, A. G. Yarmolich<sup>1, 2</sup>**

<sup>1</sup> Radioavionika, Saint-Petersburg, Russia, <sup>2</sup> Baltic State Technical University VOENMEH, Saint-Petersburg, Russia

# ASSESSMENT OF THE PEDESTRIAN NAVIGATION SYSTEM ACCURACY BY THE SIMULATION METHOD

*The general structure of the pedestrian navigation system (PNS) is presented. PNS assessment task assigned by the adopted models of inertial navigation system (INS) and pedestrian errors is being set up. Information processing algorithm of a pedestrian navigation system is considered that implements the integration of inertial sensors measurements and updating information from an external source as a biomechanical motion model. Results of simulation modeling are presented. It is demonstrated that, within the limits of the adopted models of sensor errors and pedestrian motion, the accuracy of determining the current coordinates fits into pedestrian navigation systems requirements. The directions for future research are determined: practical accuracy assessment of the system based on the real pedestrian movement data in different conditions, improvement of models and algorithms for measurement data processing.*

**Keywords:** Kalman filter, pedestrian navigation system, integration, simulation.

For citation: Kaplin A. Yu., Stepanov M. G., Yarmolich A. G. Assessment of the pedestrian navigation system accuracy by the simulation method. Radiopromyshlennost, 2017, no. 4, pp. 6–12 (In Russian).

## Introduction

Among navigational support systems for mobile ground objects, a special place is occupied by portable autonomous pedestrian navigation systems (PNSs), designed to determine current movement parameters (velocity, coordinates) of a person [1–4]. PNSs of the specialized application class (for individual military personnel, employees of the Ministry of Emergency Situations, etc.), which requires high accuracy of the navigational sighting of a pedestrian – system carrier, are of particular interest [5, 6]. The paper [5] justifies the composition and algorithm of the channel for determining the velocity and current coordinates of the PNS for pedestrian positioning on the ground. The PNS is constructed as a strapdown inertial navigation system (INS) consisting of a triaxial accelerometer, angular velocity sensor (AVS) and magnetometer, supplemented by a computer that implements the channel operation algorithm and an external source of updating information in the form of the pedestrian movement biomechanical model.

The purpose of this study is to assess the PNS accuracy, given by the accepted models of the INS and pedestrian errors in [5]. For this purpose, analytical calculations and simulation were performed, which made it possible to estimate the maximum (minimum) errors in determining the velocity and coordinates of a pedestrian. This will allow measuring the accuracy of the PNSs of this class at the potential level for the selected

models and make justified decisions on their structure and parameters during design.

## Algorithm of the simulated PNS

Detailed justification of the algorithm of the channel for determining the velocity and current coordinates of the PNS is given in [5]. The paper contains a brief summary of its main stages.

The average values  $\bar{V}_E^{\text{IHC}}(t_k)$ ,  $\bar{V}_N^{\text{IHC}}(t_k)$  of geographic components (eastern  $E$ , northern  $N$ ) and pedestrian velocity  $V_E^{\text{IHC}}(t)$ ,  $V_N^{\text{IHC}}(t)$  are calculated in the PNS by step-by-step averaging:

$$\bar{V}_E^{\text{IHC}}(t_k) = \frac{1}{T_k} \int_{t_{k-1}}^{t_k} V_E^{\text{IHC}}(\tau) d\tau, \quad \bar{V}_N^{\text{IHC}}(t_k) = \frac{1}{T_k} \int_{t_{k-1}}^{t_k} V_N^{\text{IHC}}(\tau) d\tau,$$

where  $T_k = t_k - t_{k-1}$  – is the step duration (in general, variable).

The current values of the components  $V_E^{\text{IHC}}(t)$ ,  $V_N^{\text{IHC}}(t)$  are determined by integrating the apparent linear acceleration  $a_y(t)$  (the first INS integrator):

$$V_E^{\text{IHC}}(t) = \int_0^t a_y(\tau) \sin \alpha(\tau) d\tau, \quad V_N^{\text{IHC}}(t) = \int_0^t a_y(\tau) \cos \alpha(\tau) d\tau,$$

measured by the horizontal axis of sensitivity  $OY$  of the accelerometer, coinciding with the direction of motion. Here  $\alpha(t)$  – current azimuth formed by the azimuth channel of the PNS. This channel is considered in [6], which also shows that using a rational combination of

measuring sensors and integrated data processing, it is possible to achieve high accuracy of azimuth determination. Later, when simulating the errors of the azimuth channel are not taken into account.

Step average velocities  $\bar{V}_E^{\text{IHC}}(t_k)$ ,  $\bar{V}_N^{\text{IHC}}(t_k)$  are represented by a sum (the discrete time  $t_k$  is omitted)

$$\bar{V}_E^{\text{IHC}} = \bar{V}_E + \delta V_E, \bar{V}_N^{\text{IHC}} = \bar{V}_N + \delta V_N, \quad (1)$$

where  $\bar{V}_E$ ,  $\bar{V}_N$  – are real average values;  $\delta V_E$ ,  $\delta V_N$  are slowly varying errors of the calculated values  $\bar{V}_E^{\text{IHC}}$ ,  $\bar{V}_N^{\text{IHC}}$ , caused by the leveling errors  $\beta_N$ ,  $\beta_E$  and the projections of AVS zero drifts  $\varepsilon_N$ ,  $\varepsilon_E$ . It is assumed here that the errors  $\delta V_E$ ,  $\delta V_N$  during the step are almost constant.

Using the method of approximation by Schuler oscillations (the oscillation period is 84.4 minutes), the discrete equations of the state for the errors  $\delta V_E$ ,  $\delta V_N$  will be written as follows (hereinafter, the  $t_k$  time is replaced by the  $k$  index):

$$\mathbf{x}(k) = \Phi(k, k-1)\mathbf{x}(k-1) + \mathbf{w}(k-1), k = 1, 2, \dots, K,$$

where the state vector  $\mathbf{x}(k)$  for the eastern error  $\delta V_E(k)$  is written as  $\mathbf{x}_E(k) = [\delta V_E(k), \beta_N(k), \varepsilon_N(k)]^T$ , for the northern error  $\delta V_N(k) - \mathbf{x}_N(k) = [\delta V_N(k), \beta_E(k), \varepsilon_E(k)]^T$ . The state transition matrix  $\Phi(k, k-1)$  is respectively equal to

$$\Phi_E(k, k-1) = \begin{bmatrix} 1 & -gT_k & 0 \\ \frac{T_k}{R_3} & 1 & T_k \\ 0 & 0 & 1 \end{bmatrix},$$

$$\Phi_N(k, k-1) = \begin{bmatrix} 1 & gT_k & 0 \\ -\frac{T_k}{R_3} & 1 & T_k \\ 0 & 0 & 1 \end{bmatrix},$$

where  $g$  is gravity acceleration;  $R_3$  is the radius of the Earth. The system noise vector  $\mathbf{w}(k)$  (forming the noise) is written in two versions:

- for the eastern error  $\mathbf{w}_E(k) = [w_E^a(k), 0, w_E^\varepsilon(k)]^T$ , where  $w_E^a(k)$ ,  $w_E^\varepsilon(k)$  – is Gaussian noise with zero expected value and variances  $(\sigma_E^a)^2$ ,  $(\sigma_E^\varepsilon)^2$ ;
- for the northern error  $\mathbf{w}_N(k) = [w_N^a(k), 0, w_N^\varepsilon(k)]^T$ , where  $w_N^a(k)$ ,  $w_N^\varepsilon(k)$  – is similar noise with variances  $(\sigma_N^a)^2$ ,  $(\sigma_N^\varepsilon)^2$ . The covariance matrices

$\mathbf{Q}_E$ ,  $\mathbf{Q}_N$  corresponding to the noises  $\mathbf{w}_E(k)$ ,  $\mathbf{w}_N(k)$  are written as

$$\mathbf{Q}_E = \begin{bmatrix} (\sigma_E^a)^2 & 0 & 0 \\ 0 & 0 & 0 \\ 0 & 0 & (\sigma_E^\varepsilon)^2 \end{bmatrix}, \mathbf{Q}_N = \begin{bmatrix} (\sigma_N^a)^2 & 0 & 0 \\ 0 & 0 & 0 \\ 0 & 0 & (\sigma_N^\varepsilon)^2 \end{bmatrix}.$$

The average values of the velocity components  $\bar{V}_E^{\text{BH}}(k)$ ,  $\bar{V}_N^{\text{BH}}(k)$ , formed on the basis of the pedestrian movement biomechanical model (external information) are calculated as follows:

$$\bar{V}_E^{\text{BH}}(k) = \bar{V}^{\text{BH}}(k) \sin \alpha(k), \bar{V}_N^{\text{BH}}(k) = \bar{V}^{\text{BH}}(k) \cos \alpha(k),$$

where  $\alpha(k)$  is the movement azimuth at the time the step ends;  $\bar{V}^{\text{BH}}(k)$  – is the average velocity of the step, equal to the ratio of the step length  $\Delta L(k)$  and its duration  $T_k$ :  $\bar{V}^{\text{BH}}(k) = \Delta L(k) / T_k$ . In turn, in accordance with the accepted biomechanical model in the form of a biped robot with no knees, which moves in the form of an inverted pendulum with a foot length  $l$  (foot length of a pedestrian) and a maximum step movement of the center of mass  $h(k)$ , the step length is equal to  $\Delta L(k) = 2\sqrt{2lh(k) - h^2(k)}$ , – where the movement  $h(k)$  is determined by double integration

$$h(k) = \iint_{t_{k-1}}^{t_{k-1} + \frac{T_k}{2}} a_z(\tau) d\tau$$

of vertical acceleration  $a_z(t)$ , measured by the sensitivity axis  $OZ$  of the accelerometer.

The above ratios are shown in Fig. 1. A detailed analysis of the accepted biomechanical model is given in [7].

Components  $\bar{V}_E^{\text{BH}}(k)$ ,  $\bar{V}_N^{\text{BH}}(k)$  are considered as random variables unbiased relatively to the real average values  $\bar{V}_E(k)$ ,  $\bar{V}_N(k)$ .

$$\bar{V}_E^{\text{BH}}(k) = \bar{V}_E(k) + n_E(k), \bar{V}_N^{\text{BH}}(k) = \bar{V}_N(k) + n_N(k), \quad (2)$$

where  $n_E$ ,  $n_N$  are Gaussian noises with zero expected value and variances  $(\sigma_E^n)^2$ ,  $(\sigma_N^n)^2$ , which are uncorrelated with each other and with errors of the PNS horizontal channel.

The integration of the INS and the motion model allows proceeding to the differences

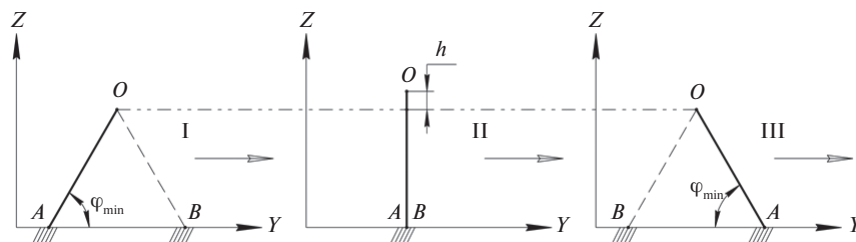


Figure 1. The test model of pedestrian traffic

$$S_E(k) = \bar{V}_E^{\text{IHC}}(k) - \bar{V}_E^{\text{BH}}(k), \quad S_N(k) = \bar{V}_N^{\text{IHC}}(k) - \bar{V}_N^{\text{BH}}(k), \quad (3)$$

which, taking into account (1), (2), are equal  $S_E(k) = \delta V_E(k) + n_E(k)$ ,  $S_N(k) = \delta V_N(k) + n_N(k)$ .

These differences are the input measurements for the Kalman filter [8], which generates optimal estimates  $\delta \hat{V}_E(k)$ ,  $\delta \hat{V}_N(k)$  of the INS error  $\delta V_E(k)$ ,  $\delta V_N(k)$ . The traditional form of the Kalman filter [9] is used, the eastern channel equations of which for this case are written as

$$\begin{aligned} \hat{\mathbf{x}}_E(k) &= \mathbf{\Phi}_E(k, k-1) \hat{\mathbf{x}}_E(k-1) + \\ &+ \mathbf{K}_E(k) [S_E(k) - \mathbf{H} \mathbf{\Phi}_E(k, k-1) \hat{\mathbf{x}}_E(k-1)], \\ \mathbf{K}_E(k) &= \mathbf{P}_E(k/k-1) \mathbf{H}^T [\mathbf{H} \mathbf{P}_E(k/k-1) \mathbf{H}^T + (\sigma_n^E)^2]^{-1}, \quad (4) \\ \mathbf{P}_E(k/k-1) &= \mathbf{\Phi}_E(k, k-1) \mathbf{P}_E(k-1) \mathbf{\Phi}_E^T(k, k-1) + \mathbf{Q}_E \\ \mathbf{P}_E(k) &= [\mathbf{I} - \mathbf{K}_E(k) \mathbf{H}] \mathbf{P}_E(k/k-1), \end{aligned}$$

where  $\hat{\mathbf{x}}_E(k) = [\delta \hat{V}_E(k), \hat{\beta}_N(k), \hat{\varepsilon}_N(k)]^T$  – is the estimate of the state vector  $\mathbf{x}_E(k)$ ;  $\mathbf{H} = [1, 0, 0]$  is the matrix (row vector) of the measurement;  $\mathbf{K}_E(k)$  is the filter gain;  $\mathbf{P}_E(k)$  is the covariance matrix of error estimates of  $\hat{\mathbf{x}}_E(k)$ ;  $\mathbf{P}_E(k/k-1)$  is extrapolated value of the matrix. The matrices  $\mathbf{\Phi}_E(k, k-1)$ ,  $\mathbf{Q}_E$  were introduced earlier.

Equations of the filter northern channel are written in a similar form.

Step-by-step update of the average velocities generated by the INS is carried out next.

$$\begin{aligned} \bar{V}_{E, \text{копп}}^{\text{ИНС}}(k) &= \bar{V}_E^{\text{ИНС}}(k) - \delta \hat{V}_E(k/k-1), \\ \bar{V}_{E, \text{копп}}^{\text{ИНС}}(k) &= \bar{V}_N^{\text{ИНС}}(k) - \delta \hat{V}_N(k/k-1), \end{aligned} \quad (5)$$

where  $\delta \hat{V}_E(k/k-1) = \mathbf{H} \mathbf{\Phi}_E(k, k-1) \hat{\mathbf{x}}_E(k-1)$ ,  $\delta \hat{V}_N(k/k-1) = \mathbf{H} \mathbf{\Phi}_N(k, k-1) \hat{\mathbf{x}}_N(k-1)$  – are extrapolated estimates of the INS error.

The final stage of the algorithm includes calculating the estimates  $\hat{E}(k)$ ,  $\hat{N}(k)$  of the current coordinates  $E(k)$ ,  $N(k)$  using the formulas

$$\begin{aligned} \hat{E}(k) &= \hat{E}(k-1) + T_k \bar{V}_{E, \text{копп}}^{\text{ИНС}}(k), \\ \hat{N}(k) &= \hat{N}(k-1) + T_k \bar{V}_{N, \text{копп}}^{\text{ИНС}}(k), \quad k = 1, 2, \dots, K, \end{aligned} \quad (6)$$

where  $K$  is the number of the last step at the pedestrian route end point.

An important component of the algorithm is the method for recording the start  $t_{k-1}$  and the end  $t_k$  of the step. A recording method is provided, in which the start (the end) of a step is defined as the moment of transition through difference zero measured by the accelerometer of the pedestrian linear acceleration vector module  $a = \sqrt{a_x^2 + a_y^2 + a_z^2}$  and acceleration of gravity  $g$  [3]. The advantage of this method is independence from the pedestrian spatial orientation (standing, lying, inclined), which is important for specialized applications. A brief

review and comparison between other methods for recording the start and the end of a step, for example, implemented in the Zero Velocity Updating (ZUPT) algorithm, are given in [10].

### Sequence and results of simulation

A phased simulation of the PNS operation was carried out in accordance with the above algorithm, including the following sequence of computational procedures:

1. Using the test motion model [7], the precise value of the average pedestrian velocity at the step (Fig. 1)  $V_y = 2l \cos \varphi_{\min} / T$  (in order to simplify the calculations, the step duration  $T_k = t_k - t_{k-1}$  is assumed constant  $T_k = T$ ) and the real average velocities (without measurement errors) are calculated

$$\begin{aligned} \bar{V}_y^{(1)} &= \frac{1}{T} \int_0^T \int_0^T a_y(\tau) d\tau, \\ \bar{V}_y^{(2)} &= \frac{2}{T} \sqrt{2l \int_0^{T/2} \int_0^{T/2} a_z(\tau) d\tau - \left( \int_0^{T/2} a_z(\tau) d\tau \right)^2}. \end{aligned} \quad (7)$$

Double integration in (7) is carried out numerically at time sampling interval  $T_{\text{д}} = 0.01$  s, corresponding to the standard data output frequency  $F_{\text{д}} = 100$  Hz by the measuring sensors (accelerometer) of the PNS. Current accelerations  $a_y(t)$ ,  $a_z(t)$  in (7) are generated during analytical calculations performed by the test model [7]. The results of calculating the velocities  $V_y$ ,  $\bar{V}_y^{(1)}$ ,  $\bar{V}_y^{(2)}$  for different values of the motion model parameters  $l$ ,  $\varphi_{\min}$ ,  $T$  indicate their practical coincidence.

Using the current azimuth  $\alpha(k)$ , the eastern and northern components of velocity  $V_y$  (real average values) are calculated:

$$\bar{V}_E(k) = V_y \sin \alpha(k), \quad \bar{V}_N(k) = V_y \cos \alpha(k). \quad (8)$$

Different sequences of the azimuth values  $\alpha(k)$ , corresponding to different pedestrian routes, were used in the simulation.

Fig. 2 shows an example of the equal distance route consisting of start, end, and five intermediate points.

The route was built using the following initial data:  $l = 0.7$  m;  $\varphi_{\min} = 60^\circ$ ;  $T = 0.5$  s. The average velocity  $V_y = 1.4$  m/s, the step length  $\Delta L = 0.7$  m, respectively. The number of steps  $K$  in the route is 10,128, which corresponds to the distance covered  $R = 7089.6$  m. The total time of the route is 84.4 minutes (1 h 24.4 minutes), that is, it coincides with the period of the Schuler oscillations. This was done to fully take into account the statistical dynamics of periodic oscillations of the INS error during their evaluation and update in the process of PNS operation.

2. Step-by-step calculation of average velocities  $\bar{V}_E^{\text{ИНС}}(k)$ ,  $\bar{V}_N^{\text{ИНС}}(k)$  (relations (1)) is carried out for various combinations of standard deviations (SD)  $\sigma_E^a$ ,  $\sigma_E^\varepsilon$ ,  $\sigma_N^a$ ,  $\sigma_N^\varepsilon$  using the accepted model of the

errors  $\delta V_E$ ,  $\delta V_N$ , real velocities (8) and a generator of normally distributed random variables. Similarly, in accordance with relations  $\sigma_E^n$ ,  $\sigma_N^n$  (2), average velocities  $\bar{V}_E^{BH}(k)$ ,  $\bar{V}_N^{BH}(k)$  are simulated for different standard deviations.

As a result, the differences  $S_E(k)$ ,  $S_N(k)$  (3) are calculated, which are fed to the input of the Kalman filter (4).

3. The accuracy of the estimates  $\delta \hat{V}_E(k)$ ,  $\delta \hat{V}_N(k)$  generated by the filter is determined by their comparison with the real values of  $\delta V_E(k)$ ,  $\delta V_N(k)$ . For this,  $M$  implementations of discrete random sequences  $\delta V_E(k, j)$ ,  $\delta V_N(k, j)$ ,  $\delta \hat{V}_E(k, j)$ ,  $\delta \hat{V}_N(k, j)$ ,  $k = 1, 2, \dots, K, j = 1, 2, \dots, M$ , were simulated, and, as a result, the average sampling expected value and the standard deviation

$$\bar{e}_E(k) = \frac{1}{M} \sum_{j=1}^M e_E(k, j),$$

$$\bar{\sigma}_E(k) = \sqrt{\frac{1}{M-1} \sum_{j=1}^M (e_E(k, j) - \bar{e}_E(k))^2}$$

of the error  $e_E(k) = \delta V_E(k) - \delta \hat{V}_E(k)$  – of the estimate  $\delta \hat{V}_E(k)$  – are calculated. Calculations for the average  $\bar{e}_N(k)$ ,  $\bar{\sigma}_N(k)$  sampling estimation  $\delta \hat{V}_E(k)$  are performed similarly.

The following are the simulation results for the motion model parameters accepted in p. 1 as applied to Fig. 2. Similar results were obtained for other initial data. Averaging was performed over  $M = 10,000$  random implementations.

Fig. 3 shows the expected values curves  $\bar{e}_N(k)$  in the first 30 steps of filtering (pedestrian movement).

With increase in  $k$ , the nature of the curves remains the same. Curves are obtained for three values of SD –  $\sigma_E^a = 0.1; 0.5; 1$  m/s at the following values of simulation parameters: initial filtration conditions –  $\delta \hat{V}_E(0) = 0.3$  m/s,  $\hat{\beta}_N(0) = 0$ ,  $\hat{\varepsilon}_N(0) = 0.1$ /s; SD of noise  $\sigma_E^e = 0.000001$  1/s,  $\sigma_E^n = 0.5$  m. The azimuth of the movement –  $\alpha = 30^\circ$  (Fig. 2).

Curves analysis shows that the estimate  $\delta \hat{V}_E(k)$  is almost unbiased ( $\bar{e}_E(k)$  close to zero). The same curves of the average sampling expected value  $\bar{e}_N(k)$  of the northern channel are of the same nature. Given

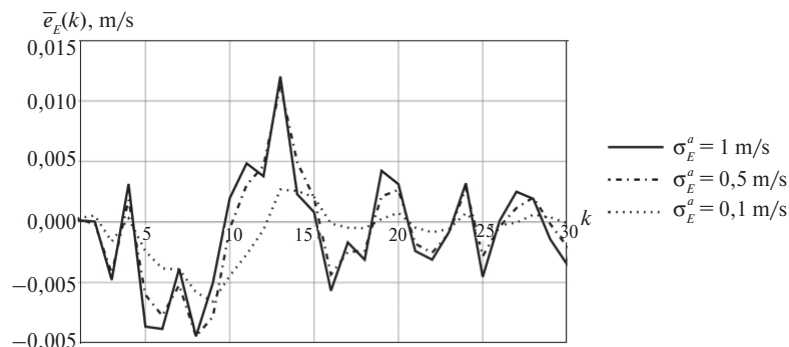


Figure 3. Expected value for the error in the eastern channel in average sample

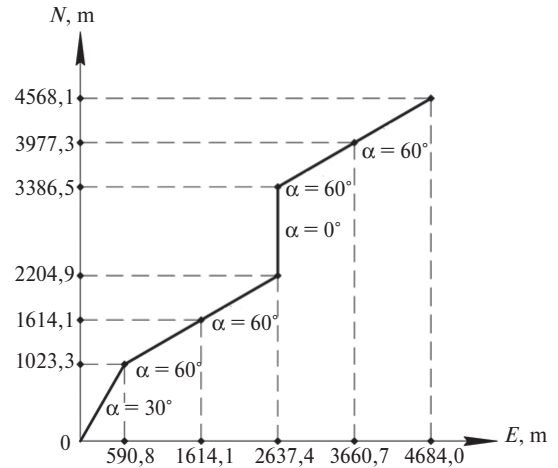


Figure 2. Example of a pedestrian route

the similarity of the results, further only the eastern channel will be considered.

Of particular interest are the SD curves  $\bar{\sigma}_E(k)$  and their comparison with the graphs of the square roots  $\sqrt{P_E(k)[1,1]}$  of the covariance error matrix  $\mathbf{P}_E(k)$  first element, which is a priori measure of the Kalman estimate accuracy  $\delta \hat{V}_E(k)$  (Figs. 4, 5). The calculations were performed for the same simulation parameters as before.

Comparison of the results leads to two important conclusions:

- First, there is a good agreement between the average sampling  $\bar{\sigma}_E(k)$  and the a priori measure  $\sqrt{P_E(k)[1,1]}$  of the Kalman filtering accuracy. This demonstrates the correspondence of the used simulation model to the analytical description of the formation and optimal estimation of INS errors.
- Secondly, the obtained numerical indicators demonstrate the possibility of achieving a high accuracy in estimating INS errors (it should be noted that in practice, the average velocity of a pedestrian is within 1.1–2.2 m/s), which ensures their effective subsequent update and the final high accuracy in

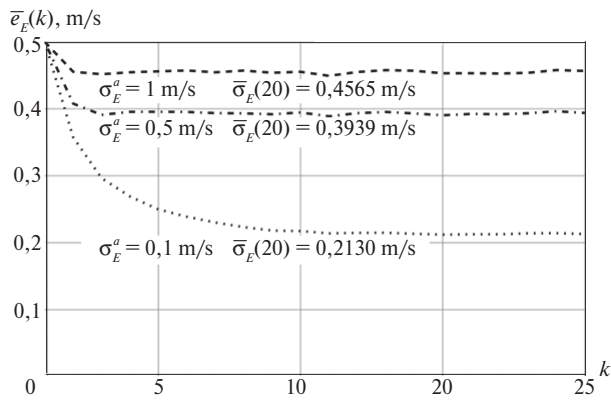


Figure 4. Plots of standard deviation in average sample  $\bar{\sigma}_E(k)$

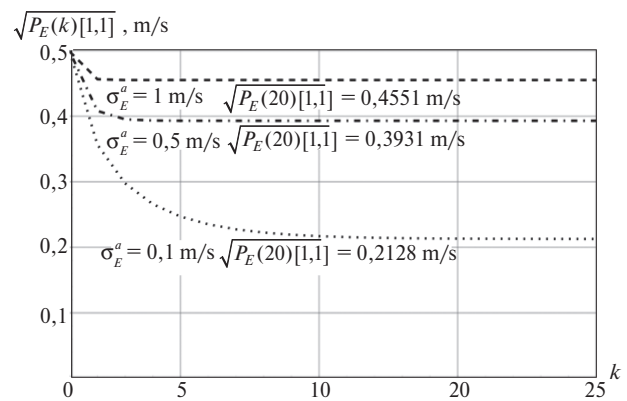


Figure 5. Square root plots  $\sqrt{P_E(k)[1,1]}$

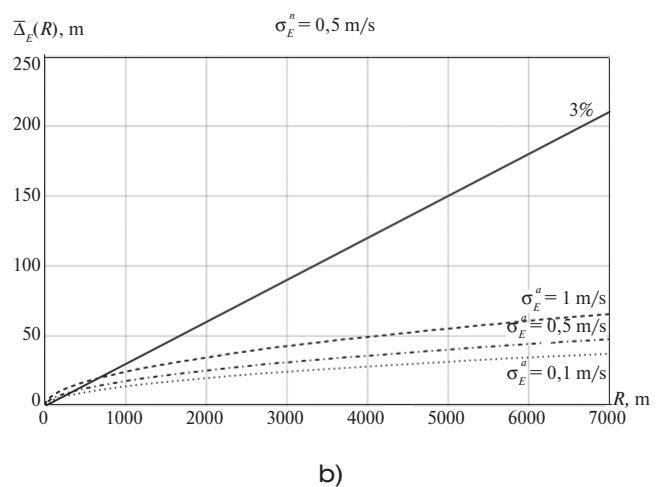
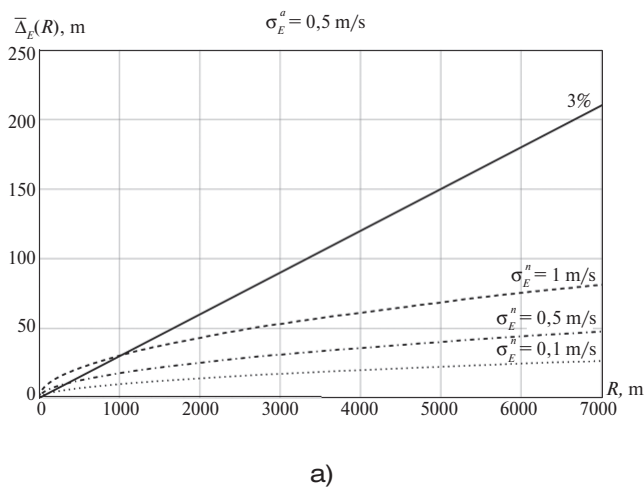


Figure 6. Dependence of the mean square positioning error  $\bar{\Delta}_E(R)$  on the travelled distance: a) for different  $\sigma_E^n$ ; b) with different  $\sigma_E^a$

determining current coordinates. This is confirmed by further simulation results.

4. The simulation is completed with the generation of the updated average velocity  $\bar{V}_{E, \text{KOPP}}^{\text{MHC}}(k)$ , by calculating the current coordinate estimate  $\hat{E}(k)$  ((5) – (6)) and calculating the average sampling value of the full root-mean-square error of pedestrian location:

$$\bar{\Delta}_E(k) = \sqrt{\frac{1}{M} \sum_{j=1}^M (E(k) - \hat{E}(k, j))^2},$$

where  $E(k)$  is the real eastern coordinate generated by the test motion model [8].

Fig. 6 shows the curves of the error  $\bar{\Delta}_E(R)$  on the distance traveled  $R$ . The initial data for the simulation and the movement route (Fig. 2) remain the same. The transition from the number  $k$  to the value  $R$  allows more clear tracing of the increase in the error of positioning during pedestrian movement and, importantly, comparing the error with the required accuracy level.

For advanced PNS, this level in steady state is 3–5% of the distance traveled for 1.5–2 hours. In Fig. 6, this corresponds to the straight line, marked with «3%». The graphs are similar for the root-mean-square error  $\bar{\Delta}_E(R)$  of the north channel.

Curve analysis in Fig. 6 shows that the considered PNS model fits in accuracy requirements with excess. It is clear that a real system, including one customized to use the model of pedestrian and INS errors, in case of real input effects (measurements) will give less accurate results. Given the large «safety factor», it should be expected that the proposed approach to the PNS construction in real conditions will provide acceptable accuracy of the pedestrian current position.

### Conclusion

The results can be used as an initial design step of the PNS for a specialized application. Further studies should be aimed at determining the achievable

accuracy of the PNS using experimental data for various variants of real pedestrian movement; rational selection of the INS measuring sensors and updating information

sources with characteristics available for the use in the PNS; improvement of models and algorithms for processing measurement information.

## REFERENCES

1. Ladetto Q., Merminod B. Digital Magnetic Compass and Gyroscope Integration for Pedestrian Navigation. *9<sup>th</sup> Sat. Petersburg Intern. conference on Integrated Navigation System*, 27–29 May 2002, Saint-Petersburg, p. 10.
2. Lukyanov V. V. Personal navigation system. *Vestnik MGTU im. N. E. Baumana*, 2006, no. 2, pp. 87–99 (In Russian).
3. Davidson P., Takala Ya. Algorithm design of the inertial navigation system by reference to specific person's manner of walking features. *Giroskopiya i navigatsiya*, 2013, no. 1, pp. 86–94 (In Russian).
4. Marinushkin P. S., Bakhtina V. A., Podshivalov I. A., Stukach O. V. [Design issues of inertial pedestrian navigation systems on MEMS-based sensor] (In Russ.) *Elektronnyi nauchny zhurnal «Nauka i obrazovanie»*, 2015, no. 6, pp. 157–173. Available at: <http://technomag.edu.ru/jour/article/view/882> (accessed 04.05.2017)
5. Kaplin A. Yu., Stepanov M. G. Using a self-contained navigation system for high accuracy pedestrian positioning in-situ. *Infomatsionno-upravlyayushchie sistemy*, 2015, no. 6, pp. 86–92 (In Russian).
6. Kaplin A. Yu., Stepanov M. G. Model and algorithm for integrated information processing of azimuth channel of the pedestrian navigation system. *Izvestiya vuzov. Priborostroenie*, 2016, vol. 59, no. 3, pp. 181–188 (In Russian).
7. Formalskiy A. M. *Peremeshhenie antropomorfnyh mehanizmov* [Movement of Anthropomorphic mechanisms]. Moscow, Nauka Publ., 1982, 368 p. (In Russian).
8. Brammer K., Ziffling G. *Filtr Kalmana-Bjusi* [Kalman-Bucy filter]. Moscow, Nauka Publ., 1982, 200 p. (In Russian).
9. Li R. *Optimalnye ocenki, opredelenie harakteristik i upravlenie* [Optimal assessments, characterization and management]. Moscow, Nauka Publ., 1966, 176 p. (In Russian).
10. Kronenvett N., Ruppelt Ya., Trommer G. F. Accurate positioning of the pedestrian in the room based on monitoring the stages of his manner of walking. *Giroskopiya i navigatsiya*, 2017, vol. 25, no. 1 (96), pp. 33–47 (In Russian).

## AUTHORS

**Kaplin Aleksandr**, PhD, chief designer, OJSC Radioavionica, 4B, Troitskiy prospekt, Saint-Petersburg, 190005, Russian Federation, tel.: +7 (812) 251-49-38, e-mail: a.kaplin@list.ru.

**Stepanov Mikhail**, Dr., professor, deputy chief designer, OJSC Radioavionica, 4B, Troitskiy prospekt, Saint-Petersburg, 190005, Russian Federation, tel.: +7 (812) 251-49-38, e-mail: smg099@mail.ru.

**Yarmolich Aleksey**, postgraduate student, Baltic State Technical University VOENMEH, 1, 1ya Krasnoarmeyskaya ulitsa, Saint-Petersburg, 190005, Russian Federation; lead engineer, OJSC Radioavionica, 4B, Troitskiy prospekt, Saint-Petersburg, 190005, Russian Federation, tel.: +7 (812) 251-49-38, e-mail: note@iarmolich.com.